DOI: 10.18462/iir.gl2026.0071

Supermarket retrofit of a refrigeration system with heat recovery and geothermal integration: A Swedish case study

Daniel STEUER*[a], Alexandre MATOS MARTINS[a], Fredrik STRENGBOHM[b], Samer SAWALHA[a], Jaime ARIAS[a]

[a] KTH Royal Institute of Technology
Stockholm, 114 28, Sweden, dsteuer@kth.se
[b] Assemblin Ventilation AB
Hägersten, 126 30, Sweden, Fredrik.Strengbohm@assemblin.se
*Corresponding author: dsteuer@kth.se

ABSTRACT

A sustainable cold chain calls for the adoption of natural refrigerants in supermarket applications, and CO_2 in a transcritical booster configuration has become an attractive solution in relatively cold climates. CO_2 transcritical refrigeration has been proven particularly efficient for heat recovery solutions. This work investigates a Swedish case study in which a refrigeration system retrofit to a CO_2 booster system with heat recovery and geothermal integration was recently implemented. The borehole installation is simultaneously used for subcooling of the refrigeration system and as heat source for the heat pump of a neighbouring residential building. The technical and economic results of the retrofit are analysed based on field measurements data, computer modelling and simulations. The results demonstrate a 14 % reduction in annual energy use from borehole subcooling and a 48 % reduction in annual energy cost from full coverage of space heating demands by heat recovery from the refrigeration system.

Keywords: Refrigeration, Case study, Heat recovery, Supermarket, Geothermal

1. INTRODUCTION

Supermarkets use about 3-4% of the yearly produced electricity in industrialized countries and have among the highest energy use per service area among commercial buildings (Gullo et al., 2018). The substantial amounts of refrigerant used in supermarkets have also caused significant direct carbon emissions through leakage during the last decades. Fluorinated carbon refrigerants are therefore being phased out under various regulations (F-gas in the EU) and replaced with low-GWP refrigerants (European Commission, 2025). CO_2 as a refrigerant for commercial refrigeration is a common natural choice and the use of transcritical CO_2 booster systems is growing rapidly in Europe (ATMOsphere, 2025). The transcritical CO_2 booster system has been shown to operate with comparable energy efficiency to its predecessors and it can also be modified to recover heat and provide air conditioning with performance comparable to those of conventional separate heat pumps or chillers (Karampour and Sawalha, 2018).

Moreover, this work investigates potential benefits of geothermal integration with supermarket refrigeration systems. An example of this is provided by the developed models of Karampour et al. (2019), demonstrating how a vertical borehole installation can be integrated as subcooler or false-load evaporator, depending on the seasonal mode of operation. In the summer season, additional subcooling reduces condenser/gas cooler exit temperatures, resulting in 3.5 % annual energy use savings in the Stockholm climate. Annual savings in energy consumption for refrigeration of about 11 % are achieved from geothermal subcooling in a similar arrangement in the Athens climate in a study by Tsimpoukis et al. (2021). In the winter/heating season, the borehole installation can instead be used as an additional heat source, through the use of a false-load evaporator, for peak heating load conditions in heat recovery mode. While the heat extraction solution does not provide any efficiency enhancements, it increases the system's capacity and resilience against peak conditions (Karampour and Sawalha, 2019; Giunta and Sawalha, 2021). In addition, the higher capacity opens up for potential surplus production and heat export to neighbouring buildings, as demonstrated by a realworld installation in Thanasoulas et al. (2023). There, the total energy costs of the supermarket and its neighbours are cut roughly in half when all thermal demands in the buildings are covered by the supermarket refrigeration system.

Another possible advantage of geothermal integration with supermarket refrigeration systems is the synergetic effect of borehole subcooling if a neighbouring building uses the same borehole installation as heat source for a heat pump. The subcooling will then not only benefit the supermarket's refrigeration system, but also the heat pump's operational conditions, as the ground will be regenerated, increasing the borehole fluid temperatures. This work investigates such a solution in a Swedish case study in the city of Örebro in central parts of Sweden.

2. CASE STUDY AND DATA COLLECTION

This manuscript is based on a M.Sc. thesis by Alexandre Matos Martins, conducted in 2025 at KTH Royal Institute of Technology, Stockholm (Sweden). For further details of this work, the reader is referred to Matos Martins (2025). The case study is provided by Assemblin Ventilation AB.

2.1. Case study

The studied supermarket ICA Parkhallen Örebro is situated in central Sweden and underwent major renovation during 2022-2024. It now has a total area of 3,000 m^2 and sales area of 2,100 m^2. A neighbouring residential building recently installed a geothermal heat pump, and during the planning of the supermarket retrofit, it was decided that the supermarket would also gain access to the boreholes as an additional heat sink to provide subcooling for their new refrigeration system. The solution provides synergetic effects, as the subcooling of the refrigeration system also regenerates the ground, thus benefitting the neighbour's heat pump by increasing the borehole fluid temperatures; see Fig. 1. The supermarket is also connected to a district heating network, which previously was the main heating system. While the connection was kept after the renovation, it is now only used for hot service water and as backup for space heating should the heat recovery system fail.

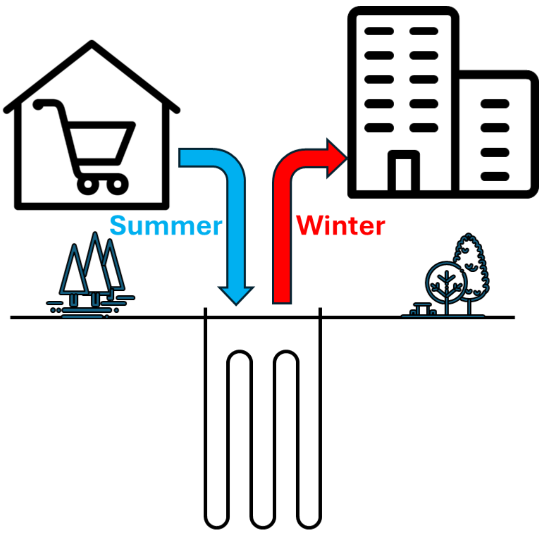

Figure 1: Simplified illustration of the shared geothermal system

The previous refrigeration system had a cascade design with direct expansion CO_2 in the low temperature (LT) stage, R513A (GWP = 573) in the medium temperature (MT) stage, and a secondary refrigerant (glycol) for distribution to the MT cabinets at temperatures of -8°C/-4°C; see Fig. 2. R513A was initially introduced as a low-GWP drop-in replacement for R134a (GWP = 1,300) and is a blend of R134a and R1234yf (Kaltra GmbH, n.d.), but future use of R513A will also be constrained by the latest version of the EU F-Gas regulation, thus motivating the latest retrofit to a pure CO2 solution.

The R513A-CO_2 cascade system maintained evaporation temperatures of -33°C (LT) and -12°C (MT), and had designed refrigerating effects for LT and MT loads of 25 kW and 130 kW, respectively. In heat recovery mode, the MT cycle operated at a fixed head pressure corresponding to a condensing temperature of 40°C, and it was connected to a heat recovery circuit serving the air handling unit (AHU), thus providing space heating. The heat recovery circuit operated at forward and return temperatures of 38°C/33°C and, while no measurements were made, it was estimated to cover less than 10 % of the annual heating demand. Prior to the renovation, the district heating use was about 400 MWh/y, and if the heat recovery estimation of 10 % is correct, the total heating demand was therefore around 400-440 MWh/y. The heat required for hot service water is currently 25 MWh/y, and it is assumed that it was nearly the same before the renovation.

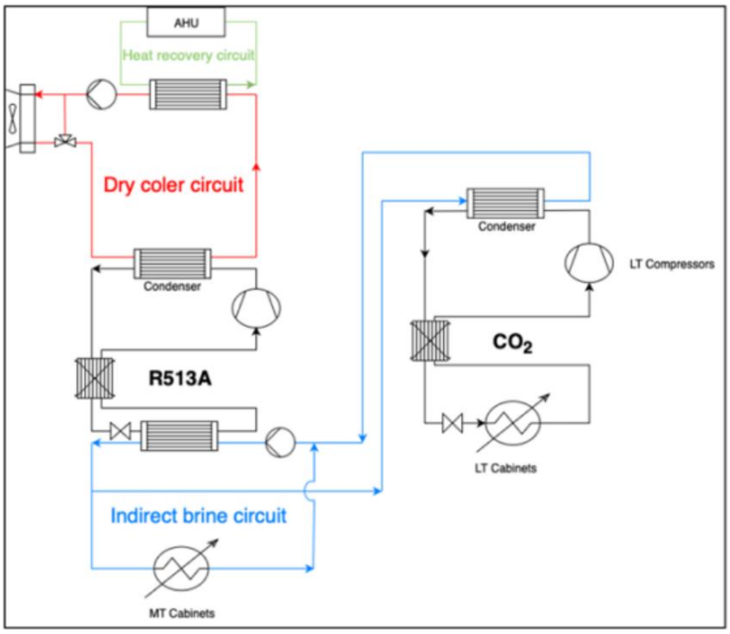

Figure 2: Previous refrigeration system solution: R513-CO_2 cascade

Due to more efficient cabinets and freezers with glass door lids, the design capacity of the refrigeration system remained unchanged after the renovation, despite an increase in number of cabinets and freezers. The current refrigeration system is a conventional CO_2 booster with geothermal integration; see Fig. 3. The principles of this system solution are generally well described in the literature and will not be explained in detail in this paper; see e.g. Karampour and Sawalha (2018) for a detailed walkthrough of the standard booster system as well as a wide range of possible modifications. The borehole heat exchanger is one such modification and it is connected in series in this case study with the two de-superheaters for heat recovery and the condenser/gas cooler. The first de-superheater is connected to radiators in the supermarket, which makes up a relatively low demand but has high required supply temperatures. The second de-superheater is connected to the AHU, as in the previous system solution, at higher capacities but lower supply temperatures.

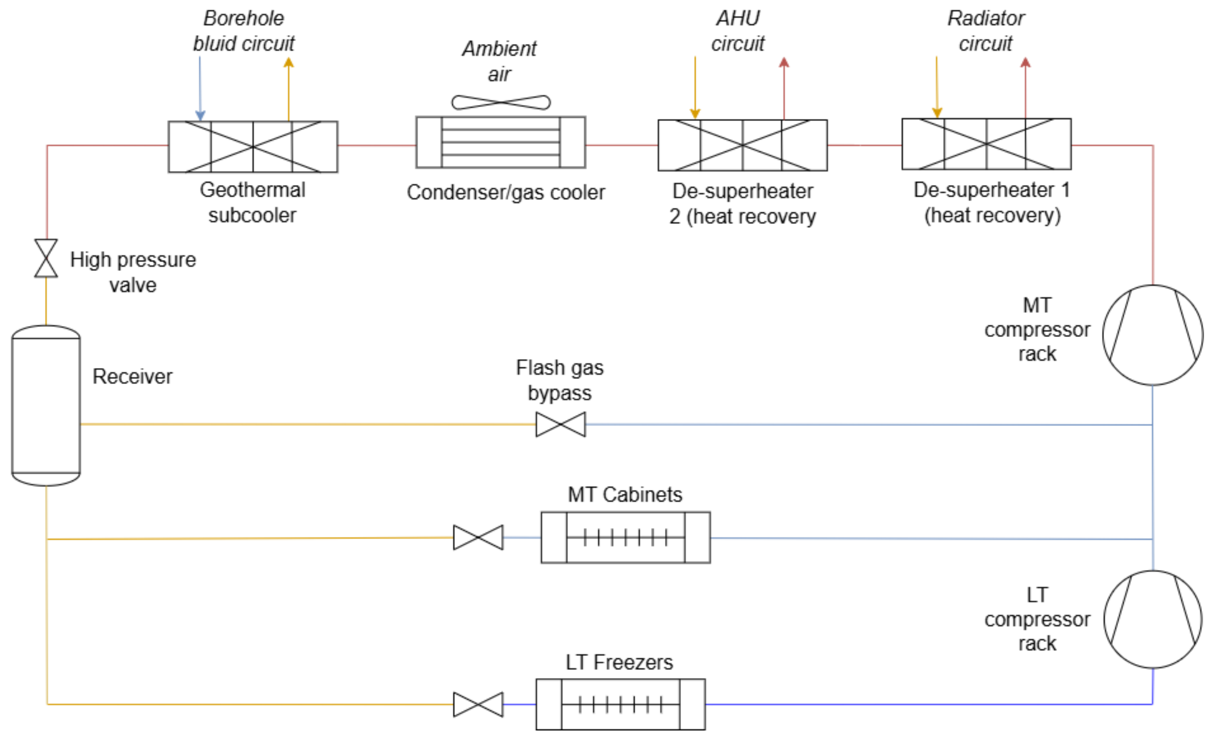

Figure 3: Current refrigeration system solution (simplified): CO_2 booster with geothermal integration

2.2. Data collection and cycle calculations

Data collection was conducted in the iTOP monitoring system by Caverion (Caverion, n.d.). Pressure and temperature sensors were installed in all cycle locations of interest and most of their data were successfully logged to the monitoring system and available for download. There were three LT compressors connected in parallel, two of which running at variable speeds and one of on-off type. Similarly, there were four MT compressors, two of which were capacity controlled. All compressors were manufactured by Dorin and their running capacities were tracked in the monitoring system. Electric power consumption was metered in aggregate for each of the two compressor racks.

Data was collected from the middle of April in 2024 to the middle of April in 2025, making up a full year of operation. The data was cleaned and processed in Microsoft Excel using forward and backward filling for missing values and the Z-score method for removal of outliers (Nevil, et al., 2025).

The CoolProp library was used in Python to determine cycle state points, such as specific enthalpy, entropy, and saturation pressure (Bell et al., 2014). The main parameters of interest which could be calculated from the collected data were cooling capacities, heat recovery, and subcooling capacity. In order to determine these parameters, the refrigerant mass flow throughout the cycle needed to be known. The mass flows were calculated using the total compressor efficiency, according to Eq. 1.

$$\dot{m}_{comp} = \frac{\dot{E}_{comp,el}}{\Delta h_{comp,is}} * \eta_{comp,tot} \qquad Equation\ (1)$$

In Eq. 1, $\dot{m}_{comp}$ is the refrigerant mass flow in kg×s^{-1} through one compressor rack, $\dot{E}_{comp,el}$ is the electric power input to the compressor rack in kW, $\Delta h_{comp,is}$ is the enthalpy difference of isentropic compression in kJ×kg^{-1}, and $\eta_{comp,tot} = f(p_{dis}/p_{suc})$ is the total compressor efficiency as a function of the pressure ratio with p_{dis} as discharge pressure (in bar) and p_{suc} as suction pressure in bar. The compressor efficiency functions were calculated as second-degree polynomials based on manufacturer data.

Mass flow balances were then performed to ensure the correct mass flows were evaluated throughout the cycle calculations. Calculating Eq. 1 at the MT compressors gives the global refrigerant mass flow $\dot{m}_{MT}$, which then separates into flash gas at the receiver, $\dot{m}_{flash}$, and saturated liquid leaving the receiver, which in turn separates into the refrigerant flowing through the MT and LT cabinets and freezers. These mass flows are denoted as $\dot{m}_{MT,cab}$ and $\dot{m}_{LT}$. The total mass balance is described by Eq. 2.

$$\dot{m}_{MT} = \dot{m}_{flash} + \dot{m}_{MT,cab} + \dot{m}_{LT} \qquad Equation\ (2)$$

In turn, $\dot{m}_{flash}$ and $\dot{m}_{MT,cab}$ are dictated by the vapor quality in the receiver, assuming isenthalpic expansion from the high pressure valve, such that $\dot{m}_{MT,cab} = \dot{m}_{MT} * (1 - X_{rec})$ and $\dot{m}_{flash} = \dot{m}_{MT} * X_{rec}$, where X_{rec} [-] is the vapor quality in the receiver. The cycle is illustrated by a pressure-enthalpy diagram in Fig. 4.

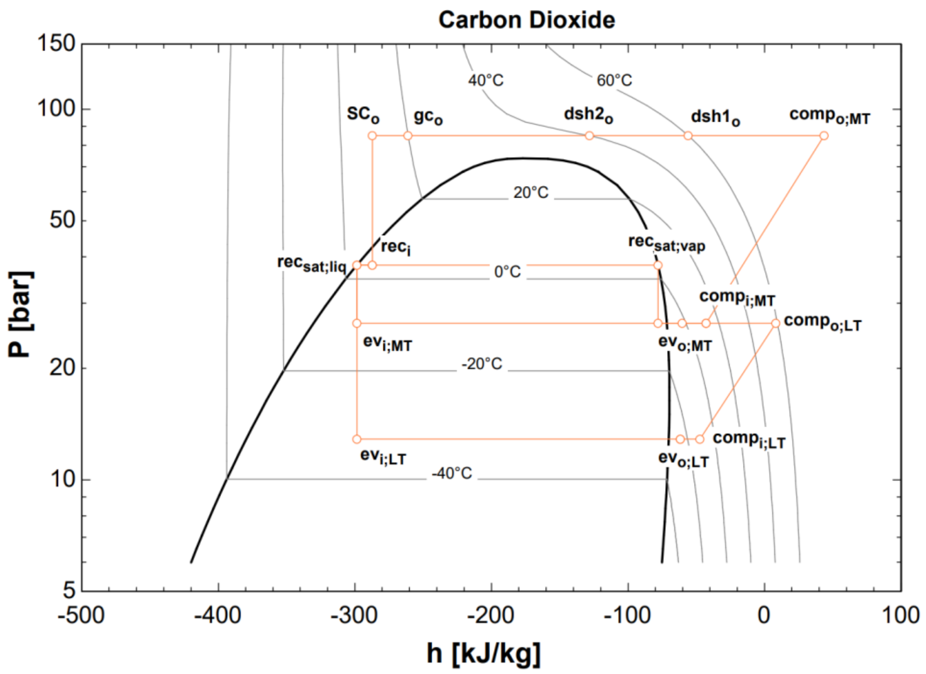

Figure 4: Pressure-enthalpy diagram of the CO_2 booster system with heat recovery and borehole subcooling

Moreover, the heat rejection process goes through four steps, of which the heat recovery and subcooling processes are of primary interest in this work. All heat rejection heat exchangers can be fully or partially bypassed by three-way valves; otherwise, they all utilize the global cycle refrigerant mass flow $\dot{m}_{tot}$. Their respective capacities are calculated by the product of the mass flow and enthalpy difference (Eq. 3):

$$\dot{Q}_{HX} = \dot{m}_{HX} * \Delta h_{HX}, \qquad Equation\ (3)$$

where $\dot{Q}_{HX}$ is the heat transfer rate in kW across a given heat exchanger, $\dot{m}_{HX}$ in kg×s^{-1} is the refrigerant flow rate, and Δh_{HX} is the enthalpy difference of the refrigerant in kJ×kg^{-1}. Eq. 3. was used to calculate all heat rejection processes, as well as the cooling capacities of the LT freezers and MT cabinets. The specific enthalpies are derived from state points based on the pressure and temperature measurements from the monitoring system.

In the absence of heat recovery, a CO_2 booster system will run in floating condensing conditions, in which the condensing temperature follows the ambient temperature with a given temperature difference, thus minimizing discharge pressure and electric power consumption. In order to recover heat, the pressure needs to be increased. The performance of heat recovery is therefore described by how much heat is recovered in relation to how much the electric power consumption of the compressor is increased. Mathematically, it is expressed by the COP_{HR}, defined as (Eq. 4):

$$COP_{HR} = \frac{\dot{Q}_{HR}}{\dot{E}_{HR} - \dot{E}_{FC}} \qquad Equation\ (4)$$

In Eq. 4, $\dot{Q}_{HR}$ is the heat recovered in both de-superheaters in kW, $\dot{E}_{HR}$ is the total electric power consumption in kW of the compressors in heat recovery operation, and $\dot{E}_{FC}$ is the total electric power consumption of the compressors in kW if they would run in floating condensing mode.

3. FIELD MEASUREMENTS CALCULATIONS AND SYSTEMS MODELLING

Computer models were developed in Python to simulate and compare the two different refrigeration systems, as well as the new one without geothermal integration. These input data and boundary conditions in the models were based on observations of the collected field measurements data.

The supermarket has been self-sufficient in terms of heating after the renovation, and the heating demand is therefore exactly equal to the heat recovery. The recovered heat in de-superheater 1 (for radiators), de-superheater 2 (for AHU), and outdoor temperatures for the period between September 2024 and March 2025 are displayed in Fig. 5. Typical values for the first and second de-superheaters, respectively, are 10-20 kW and 25-30 kW. As expected, the heating demand increases substantially during hours of very low ambient temperature, with AHU heating demand reaching values of 45-80 kW. In total, 175 MWh/y of heat are recovered by the de-superheaters, 68 % in the AHU and 32 % in the radiators. Adding the heating needed for the hot service water, the total heating demand is roughly 200 MWh/y, corresponding only to 45 % of the heating demand prior to the renovation. The MT and LT compressor racks used 175 MWh and 39 MWh of electricity respectively during the whole year of operation, with average values of about 20 kW and 5 kW. Over the year, the outdoor temperature had a minimum value of -18.1°C, maximum value of 28.6°C, and average value of 9.9°C.

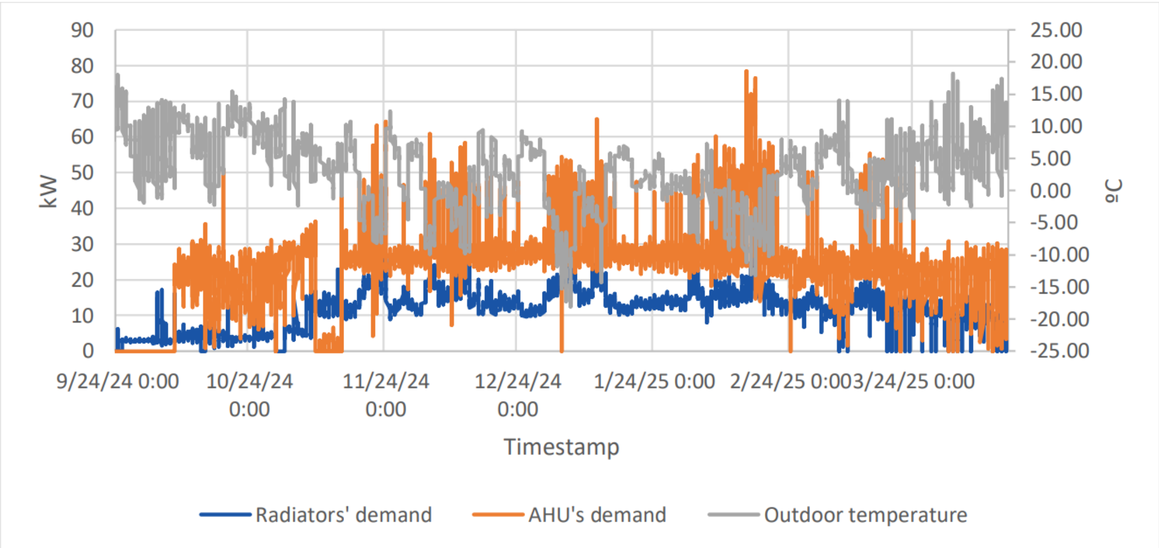

Figure 5: Field measurements data of ambient temperature and heating demand for the heating season 2024-2025

Furthermore, the borehole subcooling capacity for the period between April 2024 and March 2025 is shown in Fig. 6. The figure indicates that the control of the borehole subcooling heat exchanger was changed at several occasions during the study period. On average, the subcooling power is 28 kW and the total amount of heat rejected in the ground over the year of operation is 248 MWh. This figure can be related to the heat extraction from the ground of 440 MWh by the neighbour’s heat pump. Thus, the effect of subcooling provides a net reduction of ground heat extraction of 56 % for the neighbours. While this reduction should lead to an increase in evaporation temperature and therefore in performance of the neighbour's heat pump, the exact magnitude of this effect is not yet analysed in detail in this work.

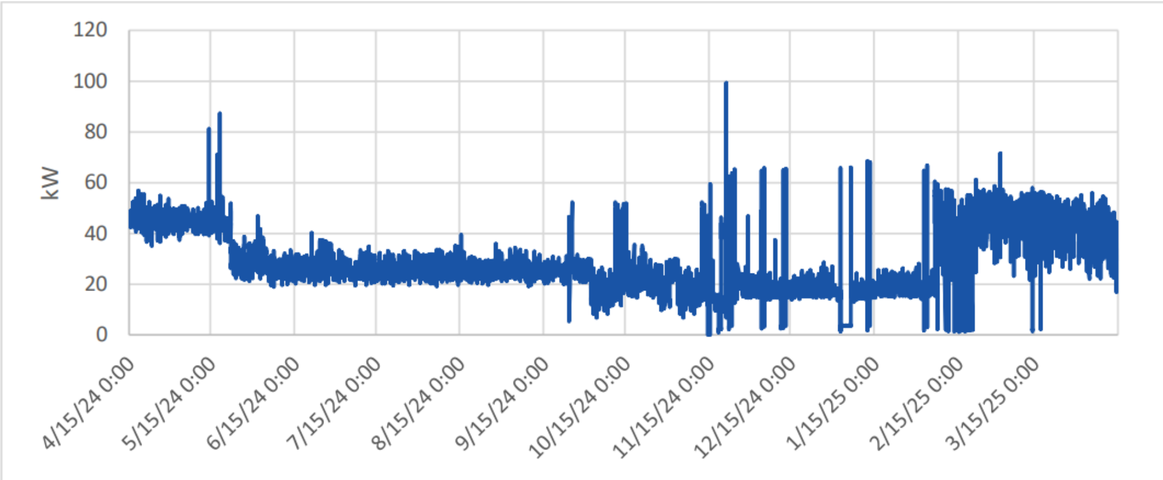

Figure 6: Metered borehole subcooling capacity for April 2024 to March 2025

3.1. Systems Modelling

After performing the field measurements calculations, the modelled scenarios were developed to assess the impact of retrofitting the refrigeration system and of integrating borehole subcooling. In order to compare them, the two refrigeration systems were modelled and simulated in Python, as no data was available from the old system. The simulations were made for one year of hourly average values in Python, and the results were post-processed in Microsoft Excel.

The thermal demands were modelled as functions of ambient temperature based on data obtained from the field measurements calculations. The heating demands for radiators and the AHU were both modelled as linear functions of the ambient temperature. The LT refrigeration load was kept constant, and the MT refrigeration load was modelled as constant during the winter and as a linear function of outdoor temperature at values above 0°C; see Fig. 7.

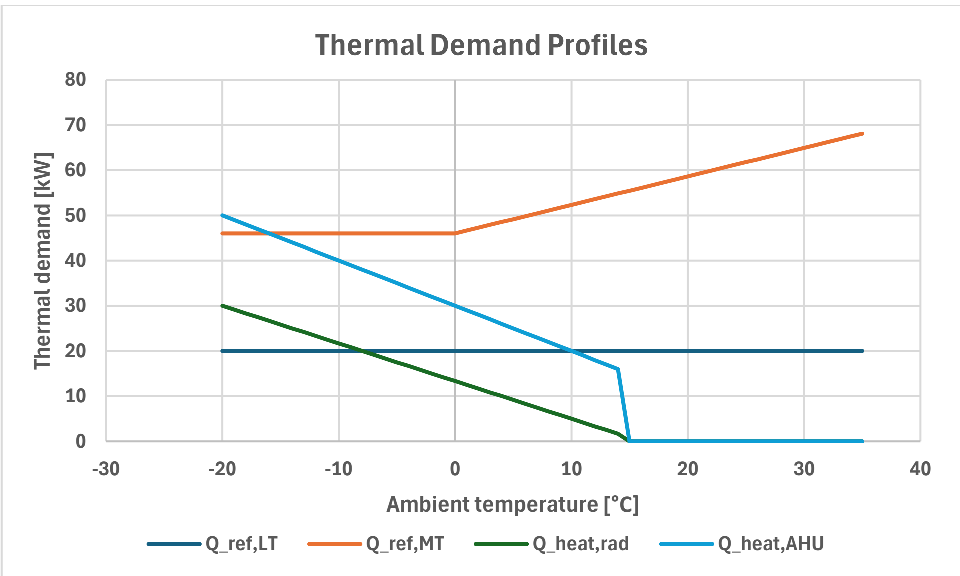

Figure 7: Thermal demands input to simulation models

The most important parameters used in modelling the systems are summarized in Table 1. Both systems were assumed to operate in floating condensing mode whenever there was no heating demand. In the R513A-CO_2 cascade system, the heat recovery operation was quite simple as it was controlled on a fixed head pressure, corresponding to a condensing temperature of 40°C. Whatever amount of heat that was available was recovered, and the remaining heating demand was assumed to be met by district heating. Due to complications in CoolProp, the refrigerant blend R513A was actually modelled as R134a. Given that R513A was developed as a drop-in substitute to R134a, their properties and performance are similar, and so it should not have a significant impact on the results.

Table 1: Key system parameters used in modelling

Parameter	R513A-CO_2 cascade	CO_2 booster
Evaporation temperature, LT [°C]	-33	-33
Evaporation temperature, MT [°C]	-12	-10
Superheat, internal/external [K]	10/0	14/8
Liquid subcooling [K]	0	Variable
Condenser/gas cooler approach [K]	7	7
Minimum condenser/gas cooler outlet temperature [°C]	10	10
LT compressor efficiency [%]	67	63
MT compressor efficiency [%]	Curve-fitted	70

By iteration of the MT discharge pressure, the CO_2 booster system was controlled to exactly cover the space heating demand. In the case of borehole subcooling, the condenser/gas cooler was partially by-passed, as long as the discharge pressure was subcritical, ensuring the vapour quality was 20 % at the borehole heat exchanger (BHE) inlet. This assumption was made iteratively to match the real heat rejected into the ground over the year of operation, 248 MWh per year. Borehole charging was in reality performed also in the winter, as indicated by Fig. 6.

In the case of no borehole subcooling, most parameters remained unchanged, the exceptions being MT discharge pressure, gas cooler outlet temperature, and mass flow rate. During the heating season, the discharge pressure was found by a new iteration to match recovered heat with the heating demand. No subcooling was assumed in subcritical temperatures, so the condenser outlet temperature was equal to the condensing temperature. In trans-critical operation the gas cooler outlet temperature was fixed at 25°C. During the summer season, the system was modelled in floating condensing conditions, assuming 7 K temperature difference between condensing and ambient temperature. In transcritical conditions, the discharge pressure was modelled to follow Eq. 5. (Sawalha, 2008):

$$p_{dis} = 2.7 * t_{gc,o} - 6.1 \qquad Equation\ (5)$$

In Eq. 5, p_{dis} is the MT discharge pressure in bar and $t_{gc,o}$ is the refrigerant temperature in °C at gas cooler outlet. Finally, the scenarios were compared by the following performance indicators: COP_{HR}, seasonal COP_{HR} ($SCOP_{HR}$), and Annual Energy Cost (AEC). The $SCOP_{HR}$ is the weighted annual average of the COP_{HR} defined in Eq. 4. AEC is calculated by Eq. 6:

$$AEC = \sum_{i=1}^{8760} E_{el,i} * P_{el} + Q_{DH,i} * P_{DH}, \qquad Equation\ (6)$$

where P_{el} is the electricity price in SEK×kWh^{-1} and P_{DH} is the district heating price in SEK×kWh^{-1}. The supermarket has a fixed rate contract for electricity with P_{el} = 0.90 SEK×kWh^{-1}, and P_{DH} = 1.25 SEK×kWh^{-1} was taken from E.ON's price structure (E.ON, 2025). Since the heating demand was reduced dramatically following the renovation, the heating costs cannot be compared directly. It is therefore assumed that both modelled scenarios have the new, lower space heating demand of 175 MWh per year. The hot water demand of 25 MWh per year also remains the same in both scenarios.

4. SIMULATION RESULTS AND DISCUSSION

The simulated version of the CO_2 booster system produced almost the same results as those obtained from field measurements calculations, with annual energy use in the MT and LT compressors differing only by +1.7 % and +2.6 %. The CO_2 booster model without borehole subcooling caused 28 MWh higher electric energy use annually compared to the old system. The higher electricity use of compressors is due increased level of heat recovery in the CO_2 booster system. Hence, the geothermal integration provides about 14 % annual energy use savings, corresponding to economic savings of roughly 25,000 SEK.

Moreover, the modelling of floating condensing operation enabled for evaluation of the COP_{HR} (defined in equation 4) in the field measurements calculations. The COP_{HR}, discharge pressure, and heating demand are plotted against outdoor temperature in Fig. 8. All plotted variables appear to follow a similar trend, namely a decrease in value with increasing outdoor temperature. This indicates that heat recovery is the most efficient at relatively high capacity and high discharge pressure; in this case, at discharge pressures around the transition region between sub- and transcritical conditions, and heating demands around 50-70 kW. There, the COP_{HR} is generally high and varies between 6 and 10. The $SCOP_{HR}$ is 6.6. At higher outdoor temperatures, the COP_{HR} fluctuates more and has lower values overall. A possible explanation for this is the elevated discharge pressures during these periods, which may not be warranted given the relatively low heating demands.

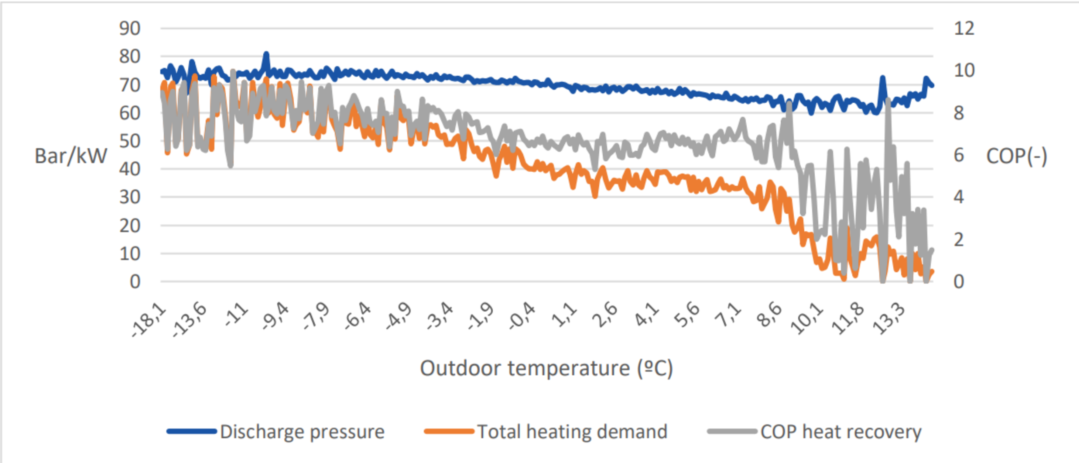

Figure 8: Heat recovery control and performance in CO_2 booster

Finally, the annual energy use of the refrigeration system in the three scenarios are calculated and illustrated by Fig. 9a. The electricity use for refrigeration in the R513A-CO_2 cascade system is higher than the CO_2 booster system with borehole subcooling, but lower than the standard CO_2 booster, demonstrating the advantage of geothermal integration. Despite lower electricity use for heat recovery, the CO_2 booster also covers the entire space heating demand, unlike the R513A-CO_2 cascade system which only covers 40 MWh, corresponding to about 23 % of the total heating demand. There, the remaining 135 MWh are covered by district heating, as shown in Fig. 9b.

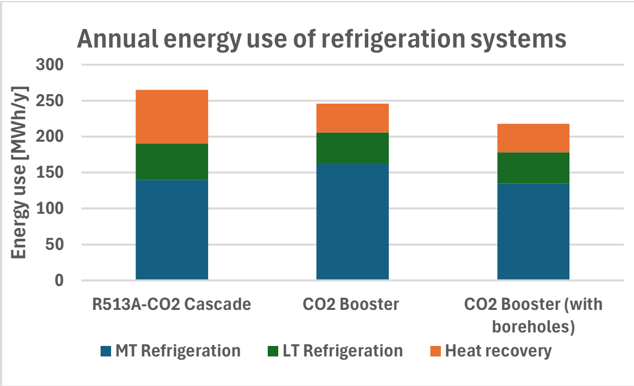

a)

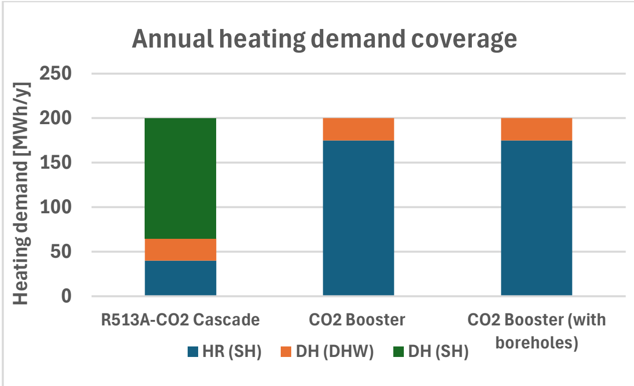

b)

Figure 9: a) Annual energy use of refrigeration system and b) annual heating demand coverage

With the assumed energy prices presented in section 3.1., the Annual Energy Costs (AEC) are calculated to 438,500 SEK for the R513A-CO_2 cascade system and 227,450 SEK for the CO_2 booster system with geothermal integration; see Fig. 10. The retrofit therefore resulted in vast economic cost savings of 211,000 SEK/y, corresponding to 48 % of the previous energy costs for refrigeration and heating in the supermarket.

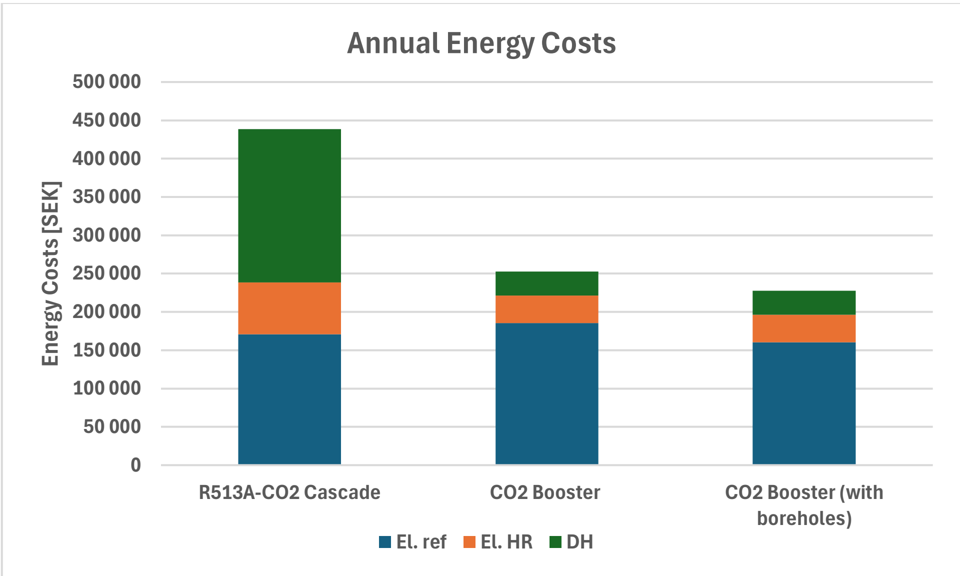

Figure 10: Annual energy costs

5. CONCLUSIONS

This work investigates the techno-economic performance of a refrigeration system retrofit in a Swedish supermarket. The case study now uses a CO_2 transcritical booster system with two-stage heat recovery and borehole subcooling. The boreholes are also used as a heat pump for a neighbouring building, and the subcooling of the refrigeration system simultaneously regenerates the ground, thus benefitting both parties.

Under present control strategies, 248 MWh of heat is inserted into the ground, reducing the refrigeration system's annual energy use by 14 %. This corresponds to roughly 10 % of the energy costs for heating and refrigeration. Simultaneously, the heat pump's net heat extraction from the ground is reduced by 56 %/year.

Moreover, the new heat recovery system is analysed and proven to be more efficient than the previous R513A-CO_2 cascade system, now covering all space heating demands in the premises at a $SCOP_{HR}$ of 6.6. The current solution yields annual economic savings of 211,000 SEK, corresponding to 48 % of the previous energy costs for refrigeration and heating.

To conclude, this case study of a Swedish supermarket demonstrates the competitive efficiency of heat recovery from transcritical CO_2 refrigeration systems in a booster configuration. The case study also sheds light on promising geothermal solutions which can provide synergies between refrigeration systems and heat pumps, opening up for collaboration between supermarkets and neighbouring buildings. Further work on the installation will investigate more in detail which subcooling/charging strategy will provide most benefits for both parties, as well as the techno-economic optimum size of the geothermal system.

Acknowledgements

The case study of this work is provided by Assemblin Ventilation AB. This research is part of the RETRO-HEAT project funded by the Swedish Energy Agency through the ReBygg research program for resource efficient buildings. RETRO-HEAT is led by Research Institutes of Sweden (RISE), and the other parties are Svenskt geoenergicentrum AB and Lund University. The project also contributes to Annex 60 in IEA's HPT Technology Collaboration Programme.

REFERENCES

ATMOsphere, 2025. Natural Refrigerants: State of the Industry 2024. Available at: https://atmosphere.cool/atmo-market-report-2024/. Accessed 2026-01-19.

Bell, I., Wronski, J., Quoilin, S., Lemort, V., 2014. Pure and Pseudo-pure Fluid Thermophysical Property Evaluation and the Open-Source Thermophysical Property Library CoolProp. Industrial & Engineering Chemistry Research 53(6), 2498-2508.

Caverion, n.d. CO2 Refrigeration revolutionises the sustainability of your property's cooling. Available at: https://www.caverion.com/catalog/services/sustainable-co2-refrigeration/. Accessed 2026-01-19.

E.ON, 2025. Fjärrvärmepris. Available at: https://www.eon.se/fjarrvarme/priser. Accessed 2026-01-19.

European Commission, 2024. F-Gas Regulation (EU) 2024/573. Available at: https://eur-lex.europa.eu/eli/reg/2024/573/oj. Accessed 2026-01-19.

Giunta, F., Sawalha, S., 2021. Techno-economic analysis of heat recovery from supermarket's CO2 refrigeration systems to district heating networks. Applied Thermal Engineering 193, 117000.

Gullo, P., Hafner, A., Banasiak, K., 2018. Transcritical R744 refrigeration systems for supermarket applications: Current status and future perspectives. Int. J. Refrigeration 93, 269-310.

Kaltra GmbH, n.d. Refrigerant R513A. Available at: https://www.kaltra.com/r-513a. Accessed 2026-01-19.

Karampour, M., Sawalha, S., 2018. State-of-the-art integrated CO_2 refrigeration system for supermarkets: A comparative analysis. Int. J. Refrigeration 86, 239-257.

Matos Martins, A., 2025. Supermarket retrofit from HFC/HFO to CO_2 booster refrigeration system: field measurements & modelling. M.Sc. thesis at KTH Royal Institute of Technology, Stockholm, Sweden.

Nevil, S., Kindness, D., Velasquez, V., 2025. Z-Score: Meaning and Formula. Investopedia. Available at: https://www.investopedia.com/terms/z/zscore.asp. Accessed 2026-01-26.

Sawalha, S., 2008. Carbon Dioxide in Supermarket Refrigeration. Doctoral Thesis at KTH Royal Institute of Technology, Stockholm, Sweden.

Thanasoulas, S., Arias, J., Sawalha, S., 2023. Investigating the heating and air conditioning provision capability of a supermarket to neighboring buildings: Field measurement analysis and economic evaluation. Applied Thermal Engineering (230), 120782.

Tsimpoukis, D., Syngounas, E., Petsanas, D., Mitsopoulos, G., Anagnostatos, S., Bellos, E., Tzivanidis, C., Vrachopoulos, M. Gr., 2021. Energy and environmental investigation of R744 all-in-one configurations for refrigeration and heating/air conditioning needs of a supermarket. Journal of Cleaner Production 279, 123234.